Microbial Biotechnology

WILEY

MICROBIAL BIOTECHNOLOGY Open Access

RESEARCH ARTICLE OPEN ACCESS

Sorbitol Uptake and Oxygen Transfer Shape *AOX1* Promoter Induction in Formate Dehydrogenase-Deficient *Komagataella phaffii*

Cristina Bustos[1,2] | Rocio Cozmar[1,2] | Julio Berrios[2] | Patrick Fickers[1]

[1]Microbial Processes and Interactions, TERRA Teaching and Research Centre, Gembloux Agro-Bio Tech, University of Liege, Gembloux, Belgium | [2]School of Biochemical Engineering, Pontificia Universidad Católica de Valparaíso, Valparaiso, Chile

Correspondence: Patrick Fickers (pfickers@uliege.be)

Received: 23 June 2025 | **Revised:** 9 September 2025 | **Accepted:** 24 October 2025

Funding: This research was funded by Becas Doctorado Nacional grant number 21211138 and 21211350 Agencia Nacional de Investigación y Desarrollo (ANID), Chile; Doctoral Internship Scholarship (PUCV, Chile); Research Stay Scholarship (Dirección de Postgrado y Programas, UTFSM, Chile); ERASMUS+ 2022–2023 Grant agreement for mobility participants—Higher education (PIC:999854952, E10208749); Wallonie-Bruxelles International through the Cooperation bilateral Belgique-Chilli project SUB/2019/435787 (RIO4), SUB/2023/591923/MOD (RI06) and SUB/2023/585456 (RC06). FONDECYT Regular (project number 1191196), University of Liege, Terra Teaching and Research Center.

Keywords: AOX1 promoter | formate | formate dehydrrogenase | *Komagataella phaffii* | oxygen transfer rate | sorbitol uptake

ABSTRACT

In *Komagataella phaffii*, the use of formate as an *AOX1* promoter (P_{AOX1}) inducer in combination with sorbitol, a non-repressive carbon source, has emerged as a promising alternative to methanol-based expression systems. Recently, we demonstrated that formate derived from the tetrahydrofolate-mediated one-carbon (THF-C1) metabolism accumulates in *K. phaffii* cells deficient in formate dehydrogenase (FdhKO) when grown in sorbitol-based methanol-free medium. Using the lipase CalB from *Candida antarctica* as a model protein, we observed that recombinant protein (rProt) productivity in an FdhKO strain grown on sorbitol was comparable to that of an Fdh-proficient strain grown on methanol. However, sorbitol is inefficiently metabolised in *K. phaffii*, leading to a low growth rate and potentially limiting rProt productivity due to insufficient energy and carbon supply. Here, we increased the sorbitol uptake rate, and thus improved sorbitol metabolism, by overexpressing the gene encoding sorbitol dehydrogenase (*SOR1*) in an FdhKO strain. Our results demonstrate that while increased sorbitol metabolism promotes biomass formation, it reduces P_{AOX1} induction, as evidenced by lower formate accumulation and decreased rProt productivity, both for intracellular eGFP and secreted proteins namely CalB lipase and glucose oxidase (Gox) from *Aspergillus niger* in *SOR1*-overexpressing strains. Additionally, oxygen availability for cells influences these dynamics, with lower oxygen transfer favouring higher P_{AOX1} induction due to increased formate accumulation in an FdhKO strain. Our data also suggest that at low oxygen transfer and low sorbitol uptake rate, the proportion of cells in an induced state increased significantly. This work provides valuable insights into the interplay between sorbitol metabolism and oxygen transfer conditions, contributing to the development of improved recombinant protein production strategies in *K. phaffii*.

Cristina Bustos and Rocio Cozmar contributed equally to this article.

1 | Introduction

The methylotrophic yeast *Komagataella phaffii* (formerly *Pichia pastoris*) is widely used as a cell factory for recombinant protein (rProt) production (Ergün et al. 2021). For this purpose, the expression system based on the alcohol oxidase 1 promoter (P_{AOX1}) has served as a benchmark for decades. The P_{AOX1} promoter is tightly repressed in the presence of glucose or glycerol but is strongly induced by methanol under non-repressive conditions. Consequently, rProt production processes are typically operated in two phases. The first phase focuses on cell growth and biomass accumulation, usually using glycerol as the carbon source, which simultaneously represses P_{AOX1}. In the second phase, following glycerol depletion, methanol is fed, either alone or co-fed with a non-repressive carbon source, to induce rProt synthesis (Ergün et al. 2021). Although methanol serves both as a carbon source and inducer, it is toxic to cells and highly flammable, presenting significant challenges for large-scale production. To overcome these limitations, methanol-free expression systems have been developed through promoter and strain engineering, or by using alternative inducers for P_{AOX1} in combination with non-repressive carbon sources (for a review, see Ergün et al. 2021). Sorbitol and formate have been identified as interesting candidates as non-repressive carbon sources (Niu et al. 2013; Carly et al. 2016) and alternative inducers for PAOX1 (Tyurin and Kozlov 2015; Jayachandran et al. 2017; Singh and Narang 2020), respectively. Sorbitol is a six-carbon polyol that is converted into fructose by sorbitol dehydrogenase after transport across the plasma membrane by a hexose transporter (Jordan et al. 2016). Fructose is subsequently phosphorylated by hexokinase before entering glycolysis (Figure S1). The *K. phaffii* growth rate on sorbitol is low ($0.03\,h^{-1}$; Niu et al. 2013; Singh and Narang 2023), with a substrate-to-biomass yield ($Y_{x/s}$) of $0.56\,g\,g^{-1}$ (Singh and Narang 2023). Sorbitol is mainly used in cofeeding processes in combination with methanol (Niu et al. 2013; Carly et al. 2016) or formate (Liu et al. 2022).

Formate is a C1 molecule with low energy content (Lv et al. 2023). In the methanol dissimilation pathway (Berrios et al. 2022), formate is generated from formaldehyde by formaldehyde dehydrogenase (Fld) and further oxidized into carbon dioxide by formate dehydrogenase (Fdh) (Hartner and Glieder 2006; Figure S2). Additionally, formate is an intermediate in the tetrahydrofolate-mediated one-carbon (THF-C1) metabolism, which plays a role in several anabolic pathways, including de novo purine synthesis (Christensen and Mackenzie 2006; Figure S3). This pathway occurs in the mitochondrion and in the cytoplasm with formate being the C1-shuttle between the two compartments. Recently, we demonstrated that formate from THF-C1 metabolism accumulates in *K. phaffii* cells deficient in formate dehydrogenase (FdhKO) when grown in a sorbitol-based methanol-free medium. This endogenous formate was shown to be sufficient to trigger P_{AOX1} induction without the need for external inducer supplementation. This finding is particularly significant because any P_{AOX1}-based expression system can be converted into a self-induced system in an FdhKO strain. When cells are cultivated in a mixture of glycerol and sorbitol, rProt synthesis initiates at the end of the exponential growth phase, upon glycerol depletion from the culture medium. Using the secreted lipase CalB from *Candida antarctica* as a model protein, comparable productivities were obtained with an FdhKO CalB strain grown on sorbitol and an Fdh-expressing CalB strain grown on methanol (Bustos et al. 2024).

Oxygen availability to cells is a critical parameter to consider when developing bioreactor processes, particularly those operated at high cell densities, such as with *K. phaffii*. Although oxygen is required in large amounts during the glycerol-based growth phase (i.e., 3.5 mol per mole of glycerol), we recently reported that low oxygen availability benefits P_{AOX1} induction in cells grown on methanol (Velastegui et al. 2023).

In *K. phaffii*, energy generation is a known bottleneck for rProt synthesis in methanol-free P_{AOX1}-based processes (Feng et al. 2022). Since the low sorbitol consumption rate ($0.02\,g\,gDCW^{-1}\,h^{-1}$; Bustos et al. 2024) by *K. phaffii* could potentially limit the energy supply and thus, rProt productivity in an FdhKO strain, we aimed to enhance sorbitol metabolism in an FdhKO strain and assess the impact on rProt productivity. Given that oxygen availability to cells can also be a limiting factor for rProt synthesis and that we previously showed it influences P_{AOX1} regulation, this parameter was also considered for strains optimized for sorbitol metabolism. Our results highlight that the combination of poor sorbitol utilization and low oxygen transfer conditions enhances formate accumulation in *K. phaffii* FdhKO cells, thereby promoting higher rProt productivity.

2 | Experimental Procedures

2.1 | Strains and Media and Culture Conditions

The *Escherichia coli* and *K. phaffii* strains used in this study are listed in Table 1 and Table S1. *E. coli* was grown at 37°C in Luria-Bertani medium (LB), supplemented with antibiotics as follows: $100\,\mu g\,mL^{-1}$ ampicillin, $50\,\mu g\,mL^{-1}$ kanamycin, or $25\,\mu g\,mL^{-1}$ zeocin. *K. phaffii* was grown at 30°C either on YPD medium ($20\,g\,L^{-1}$ glucose, $10\,g\,L^{-1}$ Difco yeast extract, and $10\,g\,L^{-1}$ Difco bacto peptone) or in YNB medium ($1.7\,g\,L^{-1}$ Difco YNB w/o ammonium chloride and amino acids, $5\,g\,L^{-1}$ NH_4Cl and, $0.4\,mg\,L^{-1}$ biotin, 100 mM potassium phosphate buffer, pH 6.0) supplemented with $10\,g\,L^{-1}$ sorbitol (YNBS), $1.75\,g\,L^{-1}$ glycerol (YNBG0), $1.75\,g\,L^{-1}$ glycerol and $1.75\,g\,L^{-1}$ sorbitol (YNBGS2), $1.75\,g\,L^{-1}$ glycerol and $3.5\,g\,L^{-1}$ sorbitol (YNBGS4) or $20\,g\,L^{-1}$ sorbitol (YNBS2). *K. phaffii* transformants were selected on YPD agar plates, supplemented with $25\,\mu g\,mL^{-1}$ zeocin (YPD-Zeo). Precultures were operated as previously described (Bustos et al. 2024). Cultures were performed in Erlenmeyer shake flasks (50 mL or 250 mL) or in microbioreactors (BioLector 2, m2p-labs, Baesweiler, Germany), using 48-well Flower plates (M2P-MTP-48B, Beckman Coulter) containing 1 mL of medium. Cultures were operated at 1000 rpm with a relative humidity of 85%. Cultures under different oxygen transfer conditions (OTC) were carried out as previously described in 250 mL Erlenmeyer flasks containing varying medium volumes to benchmark oxygen transfer coefficients (K_La) of 10, 50, and $100\,h^{-1}$ (Gorczyca et al. 2020).

3 | Construction of Plasmids and *K. phaffii* Strains

The general genetic techniques were as described elsewhere (Bustos et al. 2024). The plasmids and primers used are listed in Tables S1 and S2. The SdOE and StOE expression vectors were constructed using the GoldenPiCS system (Prielhofer et al. 2017). The gene PAS_chr1-1_0490 (*SOR1*)

TABLE 1 | *K. phaffii* strains used in this study.

Number	Names	Parental strain, genotype	References
RIY232	GS115pro	GS115, *HIS4*	Theron et al. (2019)
RIY230	Fdh eGfp	GS115, P_{AOX1}-*eGFP*	Velastegui et al. (2019)
RIY308	Fdh CalB	GS115, P_{AOX1}-*αMF-CalB*	Velastegui et al. (2019)
RIY536	FdhKO eGfp Z^+	*RIY230*, *fdh1*Δ, P_{AOX1}-*eGFP* Zeo^+	Bustos et al. (2024)
RIY537	FdhKO CalB Z^+	*RIY308*, *fdh1*Δ, P_{AOX1}-αMF-*CalB* Zeo^+	Bustos et al. (2024)
RIY540	FdhKO eGfp	RIY536, *fdh1*Δ, P_{AOX1}-*eGFP* Zeo^-	Bustos et al. (2024)
RIY561	FdhKO CalB	RIY537, *fdh1*Δ, P_{AOX1}-αMF-*CalB* Zeo^-	Bustos et al. (2024)
RIY529	SdOE	RIY232, P_{GAP}-*SOR1*	This work
RIY530	StOE	RIY232, P_{GAP}-Pp*HXT1*	This work
RIY532	St&SdOE	RIY232, P_{GAP}-*SOR1*, P_{GAP}-Pp*HXT1*	This work
RIY643	FdhKO-SdOE eGfp	RIY540, *fdh1*Δ, P_{AOX1}-*eGFP*, P_{GAP}-*SOR1*	This work
RIY562	FdhKO-SdOE CalB	RIY561, *fdh1*Δ, P_{AOX1}-*αMF-CalB*, p*GAP-SOR1*	This work
RIY655	FdhKO GOx	*fdh1*Δ, P_{AOX1}-*αMF-Gox*	Lab stock (unpublished)
RIY656	FdhKO SdOE GOx	*fdh1*Δ, P_{AOX1}-*αMF-GOx*, P_{GAP}-*SOR1*	Lab stock (unpublished)

was PCR-amplified using *K. phaffii* GS115pro genomic DNA as a template, and an internal BpiI recognition sequence in gene PAS_chr1-1_0490 (*SOR1*) was removed by overlapping PCR with primers SOR1-Fw/SOR1-Rv. In the gene PAS_chr1-4_0570 (*PpHXT1*), internal BpiI and BsaI recognition sequences were removed through in silico design by selecting alternative commonly used synonymous codons, and the synthetic gene was designed with the addition of an external BsaI recognition sequence. The corresponding synthetic DNA fragment was obtained from Eurofin Genomic (Ebersberg, Germany). The resulting PCR products and the synthetic gene fragment were cloned into plasmid A2 (BB1-23) at the BsaI restriction site, yielding plasmids RIE341 (A2_BB1_23_*SOR1*) and RIE343 (A2_BB1_23_Pp*HXT1*), respectively. Positive constructs were verified by colony and plasmid PCR with M13-Fw/M13-Rv. Plasmids RIE354 (P_{GAP}-*SOR1*-ScCYC1tt) and RIE355 (P_{GAP}-Pp*HXT1*-ScCYC1tt) were assembled by Golden Gate assembly from the plasmids A4 (BB1_12_P_{GAP}), C1 (BB1_34_ScCYC1tt), D12 (BB3aZ_14), with RIE341 and RIE343, respectively, using BpiI as the restriction enzyme. The correctness of the assembly constructs was verified by colony and plasmid PCR with the primer pair pGAPInt-Fw/ScCYC1tt.Int-Rv.

The Loxp-Zeo-Loxp was released from plasmid D12 (BB3aZ_14) by HindIII and PstI restriction and cloned at the corresponding site of the C12 (BB3aK_AC) biobrick to yield plasmid RIE370 (BB3-AC-LoxP-Zeo-loxP). The double overexpression of *SOR1* and Pp*HXT1* was performed in three steps. First, plasmid RIE372 (BB2_AB-P_{GAP}-*SOR1- SsCy1*tt) was obtained by assembly of parts from plasmids RIE341, A4, C1, and D4 using BsaI as the restriction enzyme. Second, plasmid RIP374 (BB2_BC1-P_{GAP}-Pp*HXT1-RPS3*tt) was obtained by assembly of parts from RIE378, A4, C9 and D5 using BsaI. Finally, plasmid RIP378 (BB3a-P_{GAP}-*SOR1*-SsCy1tt, P_{GAP}-Pp*HXT1*-RPS3tt) was obtained by assembly of parts from RIE372, RIE374, and RIE370 with BpiI. Plasmid construct confirmation was performed with colony and plasmid PCR with the primer pairs pGAP.Int-Fw/ScCYC1tt.Int-Rv, and. Int-Fw/Rps3tt.Int-Rv respectively.

The construction of yeast strains RIY230 (Fdh eGfp), RIY308 (Fdh CalB), RIY536 (FdhKO eGfp Z^+), RIY537 (FdhKO CalB Z^+), RIY540 (FdhKO eGfp) and RIY561 (FdhKO CalB) is described elsewhere (Velastegui et al. 2019; Bustos et al. 2024). Strains RIY529 (P_{GAP}-*SOR1*-SsCy1tt, hereafter SdOE strain), RIY530 (P_{GAP}-Pp*HXT1*-SsCy1tt, hereafter StOE strain) and RIY532 (P_{GAP}-*SOR1*-SsCy1tt, P_{GAP}-Pp*HXT1*-SsCy1tt, hereafter St&SdOE strain) were obtained by transformation of strain RIY232 with AscI linearized plasmids RIP354 (P_{GAP}-Pp*HXT1*-SsCy1tt), RIP355 (P_{GAP}-*SOR1*-SsCy1tt) and RIP378 (P_{GAP}-*SOR1*-SsCy1tt, P_{GAP}-Pp*HXT1*-RPS3tt), respectively. Overexpression of *SOR1* in the RIY540 (FdhKO eGfp) and RIY561 (FdhKO CalB) strains was performed by transformation with AscI linearized plasmid RIP355 (BB3-P_{GAP}-*SOR1-SsCy1*tt) to yield strains RIY643 (*fdh1*Δ, P_{AOX1}-e*GFP*, P_{GAP}-*SOR1*, hereafter FdhKO-SdOE eGfp strain) and RIY562 (*fdh1*Δ, P_{AOX1}-αMF-*CalB*, P_{GAP}-*SOR1*, hereafter FdhKO-SdOE CalB strain). The genotypes of RIY529, RIY530, RIY532, RIY643, and RIY564 strains were verified by PCR using the primers pGAP.Int-Fw/ScCYC1tt.Int-Rv, and pGAP.Int-Fw/Rps3tt.Int-Rv, which annealed within the P_{GAP}, ScCYC1tt, and Rps3tt regions, respectively. A schematic representation of the strain genotype is presented in Figure S6.

4 | Analytical Methods

The cell growth was monitored either by optical density at 600 nm (OD_{600}) or dry cell weight (DCW). An OD_{600} value of 1 was found to correspond to 0.65 gDCW L^{-1}. Sorbitol and glycerol concentrations were determined using high-performance

liquid chromatography (Agilent 1100 series equipped with UV) (210 nm) and RID detector (Agilent Technologies, Santa Clara, CA, USA) using an Aminex HPX-87H ion-exclusion column (300 × 7.8 mm Bio-Rad, Hercules, CA, USA). Compounds were eluted from the column at 65°C with a flow rate of 0.5 mL min^{-1} and using a 5 mM H_2SO_4 solution as the mobile phase.

The intracellular eGFP fluorescence was quantified using a BD Accuri C6 Flow Cytometer (BD Biosciences, San Jose, CA, USA), as described elsewhere (Sassi et al. 2016; Bustos et al. 2024). Briefly, 20,000 cells were analysed for each sample using the FL1-A and FSC channels, and FL1-A/FSC dot plots were analysed using the CFlowPlus software (Accuri, BD Biosciences). A threshold of 5800 fluorescence units (FU) on FL1-A channel was applied to eliminate the noise for endogenous fluorescence from the cells. To calculate the total value of fluorescence in the cell population, the FL1-A median value (i.e., the eGFP fluorescence) was multiplied by the fraction of cells with eGFP fluorescence (i.e., induced cells). It was expressed in total fluorescence unit (TFU). During cultures in microbioreactors, every 10 min, biomass was monitored by light scattering at 600 nm (gain set at 2) while fluorescence was quantified at 520 nm (excitation 488 nm, gain set at 4). The eGFP fluorescence was expressed as specific fluorescence (sFU). For that purpose, fluorescence values were divided by the biomass values. The specific fluorescence value of the parental strain GS115pro was subtracted from the specific fluorescence of eGFP-producing strains to normalise the data.

The format concentration in the culture supernatant was measured using the formic acid assay kit (Megazyme Inc., Bray, Ireland) according to the manufacturer's instructions. Briefly, formate is converted into carbon dioxide by formate dehydrogenase with the formation of NADPH that is quantified at 340 nm. Formate concentration is deduced from a calibration curve.

The lipase activity in the culture supernatant was determined by monitoring the hydrolysis of p-nitrophenylbutyrate (p-NPB), following the protocols detailed elsewhere (Fickers et al. 2003). The release of para-nitrophenol was monitored at 405 nm. One unit of lipase activity was defined as the amount of enzyme releasing 1 μmol p-nitrophenol per minute at 25°C and pH 7.2 ($\varepsilon PNP = 0.0148\ \mu M^{-1}.cm^{-1}$).

The glucose oxidase (Gox) activity was monitored using a glucose oxidase assay kit (Megazyme Inc., Bray, Ireland) according to the manufacturer's instructions. Briefly, Gox catalyses the oxidation of β-D-glucose to D-glucono-δ-lactone with the concurrent release of hydrogen peroxide. In the presence of peroxidase, the H_2O_2 generated is converted, in the presence of p-hydroxybenzoic acid, into quinoneimine which is measured at 510 nm. Gox activity is calculated based on a standard curve.

For format and enzymatic assay, absorbance at specific wavelengths was monitored over time using a SpectraMax M2 (Molecular Devices, San Jose, CA, USA). All assays were conducted in triplicates.

5 | Calculations of Cultivation Kinetic Parameters

Growth rate was calculated as

$$\mu = \frac{dX}{dt}$$

where X is the biomass (gDCW/) and t is the time (h).

The specific sorbitol uptake rate was calculated as

$$qs = \frac{d[sorbitol]}{dX.t}$$

where [*sorbitol*] is the sorbitol concentration, X the biomass (gDCW/L) and t is the time (h).

6 | Results and Discussion

6.1 | Overexpression of the Sorbitol Dehydrogenase Encoding Gene Increases the Sorbitol Uptake Rate

In *K. phaffii*, low energy generation is known as a limitation for rProt production in methanol-free processes based on the P_{AOX1} (Feng et al. 2022). During the rProt production phase, sorbitol is one of the most widely used co-substrates (Çelik et al. 2009; Niu et al. 2013; Carly et al. 2016). Unfortunately, the ability of *K. phaffii* to catabolise sorbitol is low, potentially limiting the energy and carbon provision required for rProt synthesis. Sorbitol transport across the plasma membrane and its conversion to fructose by sorbitol dehydrogenase (Figure S1) has been identified as a potential bottleneck in sorbitol assimilation (Akentyev et al. 2023). The genes encoding these proteins have not yet been reported in *K. phaffii*. In *Saccharomyces cerevisiae*, the hexose transporter Hxt15 has been identified as a versatile polyol transporter, including for sorbitol (Jordan et al. 2016). Additionally, the gene encoding sorbitol dehydrogenase (Sdh, *SOR1*) has been characterised in both *S. cerevisiae* and *Komagataella kurtzmanii* (Toivari et al. 2004; Akentyev et al. 2023). A protein BLAST search using the translated *SOR1* and *HXT15* sequences from *S. cerevisiae* as queries highlighted the genes PAS_chr1-1_0490 (*SOR1*, 55.6% identity) and PAS_chr1-4_0570 (*PpHXT1*, 51% identity) as putative Sdh and Hxt candidates, respectively (Figures S4 and S5).

To increase the sorbitol uptake rate, these two genes were expressed under the control of the constitutive GAP gene promoter (P_{GAP}), either individually or in combination, in the GS115pro strain, a prototrophic derivative of strain GS115 (Table 1). In the resulting StOE strain (P_{GAP}-*PpHXT1*), the sorbitol uptake rate and cell growth rate increased by 1.7 and 1.2-fold, respectively, compared to the parental GS115pro strain (Table 2). For the SdOE strain (P_{GAP}-*SOR1*), these rates were enhanced by 5.0 and 3.3-fold, respectively. However, for the St&SdOE strain, which co-expressed both genes (P_{GAP}-*SOR1*, P_{GAP}-*PpHXT1*), the sorbitol uptake rate and cell growth rate were not further enhanced compared to the SdOE strain (1.06 and 1.03-fold, respectively). These findings demonstrate that the expression of the *SOR1* gene alone can overcome the limiting step of sorbitol assimilation in *K. phaffii*.

6.2 | Enhancing Sorbitol Metabolism Decreases P_{AOX1} Induction in FdhKO Strains on Methanol-Free Medium

In many rProt production processes, glycerol is commonly used as a carbon source for biomass formation, while a P_{AOX1} non-repressive carbon source, such as sorbitol, is preferred during the rProt synthesis phase (Ergün et al. 2022). Therefore, biomass and eGFP fluorescence were monitored for strains FdhKO eGfp (*fdh1*Δ, P_{AOX1}-*eGFP*) and FdhKO SdOE eGfp (*fdh1*Δ, P_{AOX1}-*eGFP*, P_{GAP}-*SOR1*) grown in microbioreactors in media containing glycerol and sorbitol in different ratios (1:0, 1:1, 1:2; YNBG0, YNBGS2, and YNBGS4 medium, respectively; Figure 1). Both strains exhibited diauxic growth, consuming glycerol within the first 8 h of culture, followed by a sorbitol consumption phase (Figure S7). While both strains grew similarly on glycerol, marked differences were observed during the sorbitol consumption phase for the FdhKO eGfp and FdhKO SdOE eGfp strains (e.g., 0.035 ± 0.001 and $0.129 \pm 0.001\ h^{-1}$ on YNBGS4 medium, respectively). This confirms that the overexpression of *SOR1* increases the rate of carbon assimilation and energy generation in *K. phaffii* grown on sorbitol.

TABLE 2 | Effects of *SOR1* and *PpHXT1* genes overexpression on specific growth rate and the specific consumption rate of sorbitol.

Strains (genotypes)	μ (h^{-1})	q_S (g gDCW^{-1} h^{-1})
GS115pro (GS115 prototroph)	0.036	0.03
StOE (P_{GAP}-Pp*HXT1*)	0.042	0.05
SdOE (P_{GAP}-*SOR1*)	0.119	0.15
St&SdOE (P_{GAP}-*SOR1*, P_{GAP}-Pp*HXT1*)	0.122	0.16

Note: These cultures were performed in triplicate 250 mL flasks containing 25 mL of medium. Standard deviations were less than 10% of the presented mean values.
Abbreviations: μ, specific growth rate; DCW, dry cell weight; q_s, specific sorbitol uptake rate.

Upon glycerol depletion in YNBG0 medium (in the absence of sorbitol), the specific fluorescence signals increased slightly within the same range for both the FdhKO eGfp and FdhKO SdOE eGfp strains (i.e., between 0.015 and 0.014 sFU), likely due to the derepression of P_{AOX1} following glycerol depletion. Conversely, in sorbitol-containing media (YNBGS2 and YNBGS4), eGFP-specific fluorescence markedly increased for the FdhKO eGFP strain, reaching maximal values of 0.060 and 0.065 sFU, respectively. In contrast, the increase was less pronounced in the FdhKO SdOE eGfp strain, with maximal values of 0.032 and 0.028 sFU, respectively. These findings

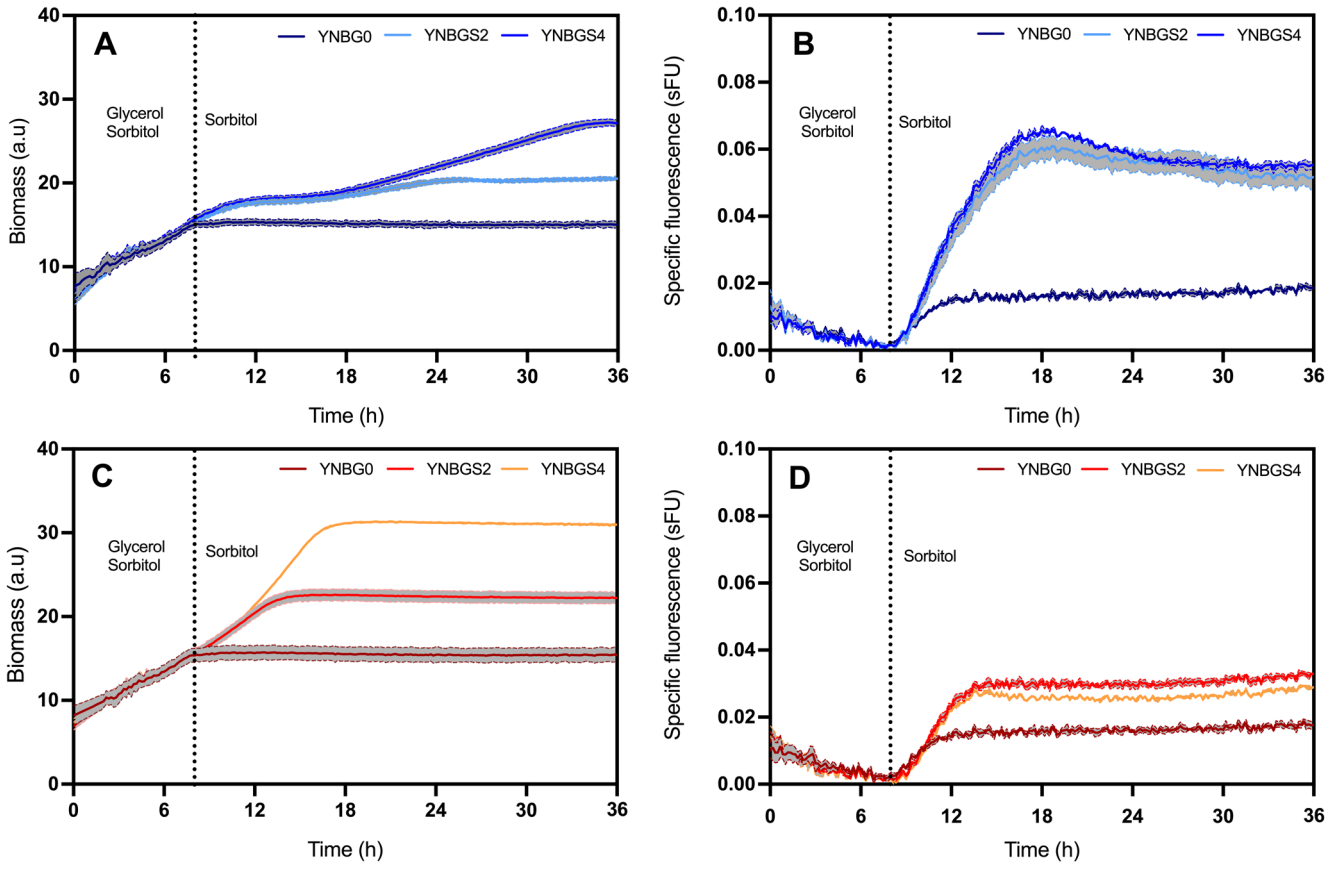

FIGURE 1 | Biomass (panels A and C) and specific fluorescence (panels B and D) during the growth of FdhKO eGfp strain (blue colours) and FdhKO SdOE eGfp strain (orange colours) in YNB minimal medium containing different mixtures of glycerol and sorbitol (1:0, 1:1, 1:2; medium YNBG0, YNBGS2, and YNBGS4, respectively). Cells were grown in a BioLector system, and data represent the mean and standard deviation (grey shade) of triplicate cultures. a.u, arbitrary units; sFU, specific fluorescence unit.

highlight that p*AOX1* induction is lower at higher sorbitol uptake rates (i.e., upon *SOR1* expression) and that sorbitol concentration does not significantly impact the strength of P_{AOX1} induction.

Similar experiments were conducted using two secreted enzymes, lipase B (CalB) from *Candida antarctica* and glucose oxidase (GOx) from *Aspergillus niger*, as model proteins. Cell growth and respective enzyme activities, namely lipase or glucose oxidase, were quantified for strains FdhKO CalB (*fdh1*Δ, P_{AOX1}-*αMF-CALB*), FdhKO SdOE CalB (*fdh1*Δ, P_{AOX1}-*αMF-CALB*, P_{GAP}-*SOR1*), FdhKO GOx (*fdh1*Δ, P_{AOX1}-*αMF-GOX*) and FdhKO SdOE GOx (*fdh1*Δ, P_{AOX1}-*αMF-GOX*, P_{GAP}-*SOR1*) grown on sorbitol in shake flasks (Figure 2). After 36 h of culture, both FdhKO SdOE strains showed higher biomass compared to their non-*SOR1*-expressing counterparts, with increases of 4.8 and 6.7-fold observed for the CalB and GOx expressing strains, respectively (Figure 2A,C). In contrast, these strains exhibited a 3.5 and 3.6-fold decrease in specific lipase and glucose oxidase activities, respectively, compared to their FdhKO counterparts (Figure 2B,D). These results for the secreted proteins align with the trend observed in the eGFP strains (i.e., FdhKO eGfp and FdhKO SdOE eGfp strains, Figure 1).

6.3 | Low Oxygen Transfer Conditions Favour the Induction of P_{AOX1} of FdhKO Strains Grown on Sorbitol-Based Methanol-Free Medium

Low oxygen availability has been reported to positively influence P_{AOX1} induction for cells grown on methanol (Velastegui et al. 2023). This has also been reported for Fab-producing strains grown under carbon-limited conditions at different oxygen supplies (Carnicer et al. 2009). To examine a similar effect on sorbitol media, FdhKO eGfp and FdhKO SdOE eGfp strains were cultivated under different oxygen transfer conditions (OTC). This was achieved by varying the ratio between volumes of the culture medium and the culture flask, yielding culture systems characterized by different volumetric oxygen transfer coefficients (K_La; Gorczyca et al. 2020). K_La values of 10, 50, and 100 h^{-1} were used as benchmarks for low, medium, and high OTC levels, respectively.

The biomass values were measured at mid-exponential growth phase (i.e., after 22 h), and the average growth rate was calculated (Figure 3A). For the FdhKO eGfp strain, the growth rate was within the same range for all culture conditions tested with an average value of 0.028 mgDCW $(mL\,h)^{-1}$ on average (Figure 3A). Conversely, significant differences were observed for the FdhKO

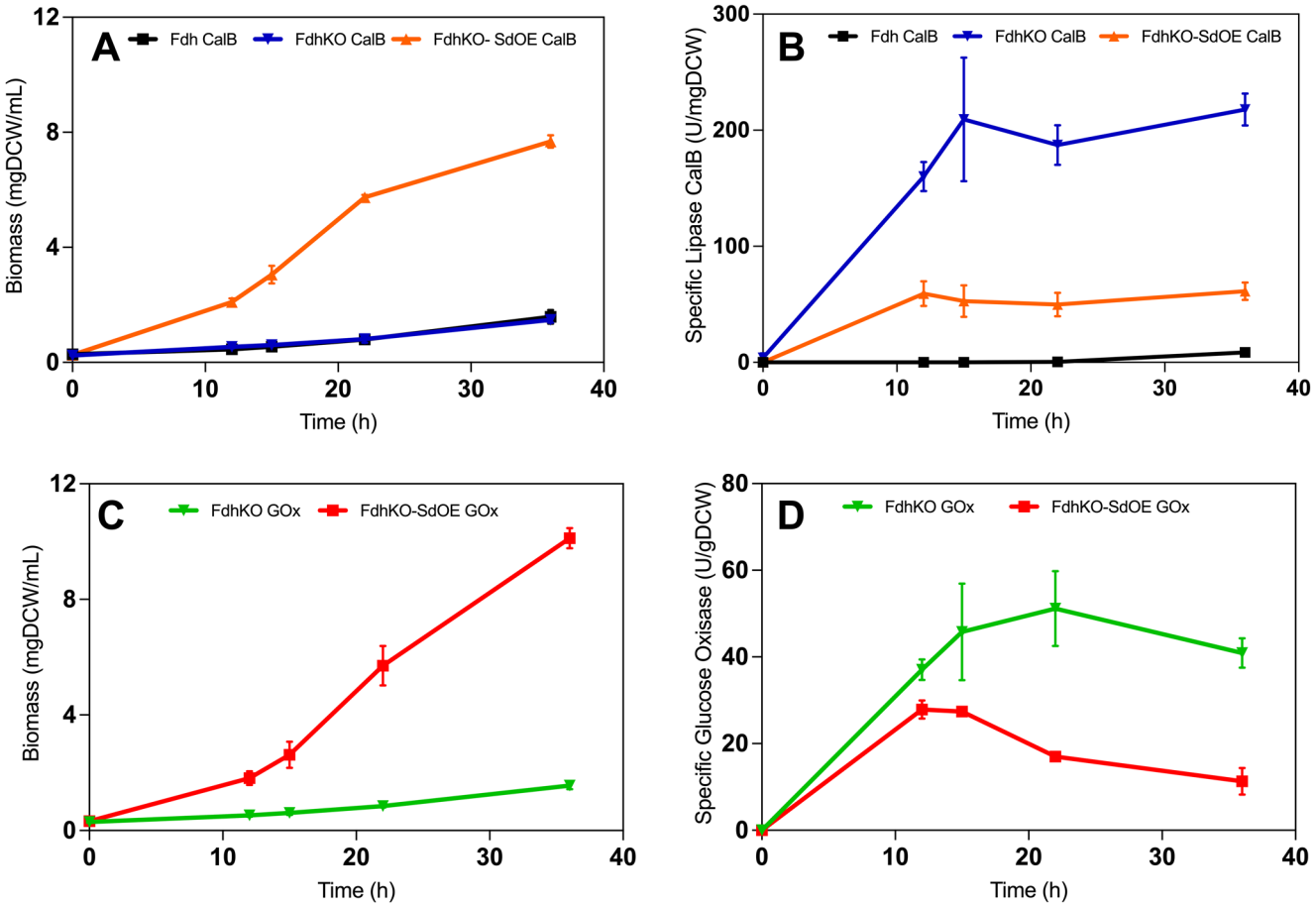

FIGURE 2 | Biomass (panel A and C) and specific enzyme activity (panel B and D) during growth of Fdh CalB (black), FdhKO CalB (blue), FdhKO GOx (green), FdKO SdOE CalB (orange) and FdKO SdOE GOx (red) strains on YNB minimal medium containing sorbitol (YNBS). Data are the mean and standard deviation of triplicate cultures conducted in shake flasks. Lipase and glucose oxidase assays were performed in triplicates.

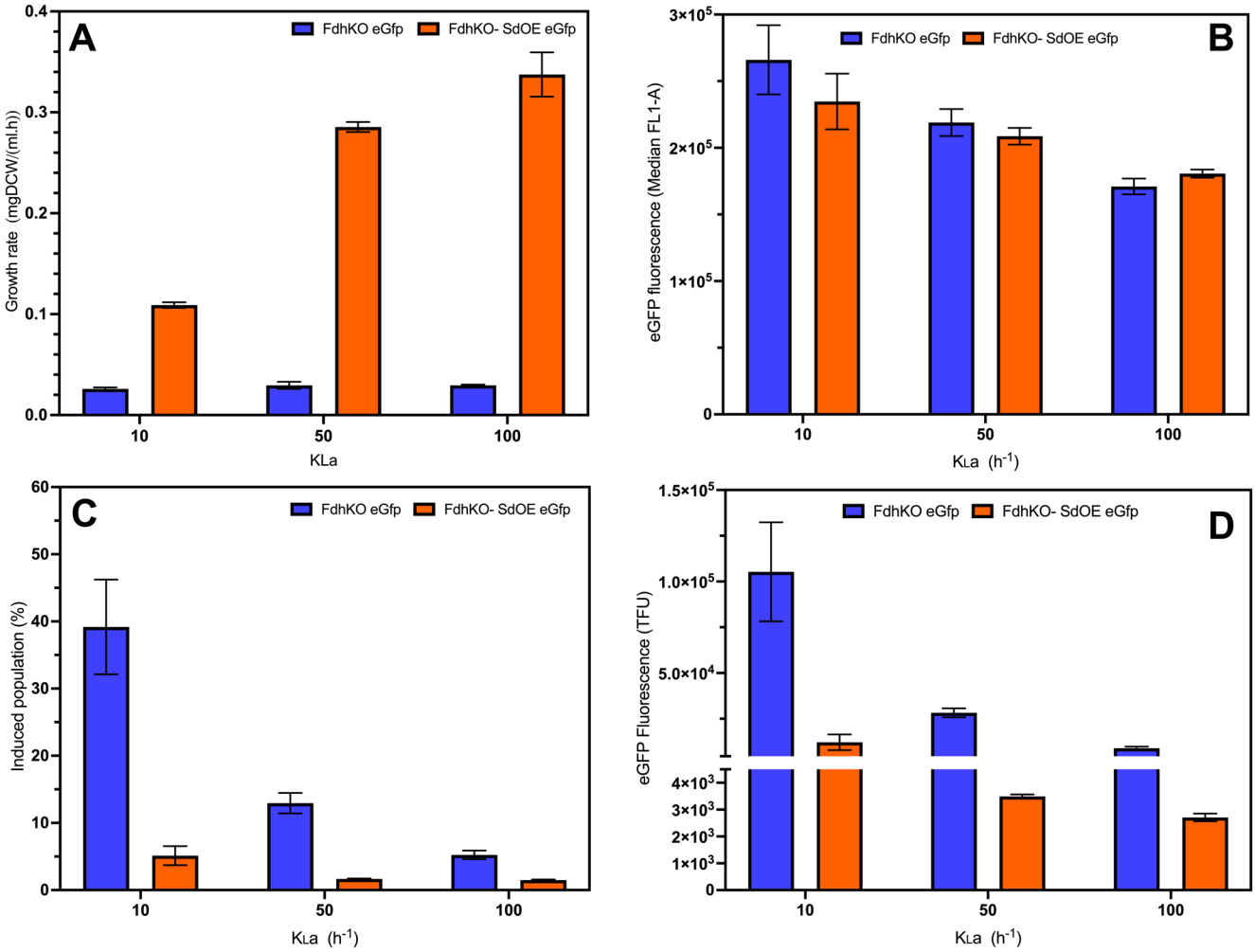

FIGURE 3 | Growth rate (panel A), Median FL1-A (panel B), induced population (panel C) and specific eGFP fluorescence (panel D) for FdhKO eGfp and FdhKO-SdOE eGfp strains cultured in YNBS2 under different OTC (low, K_La 10 h^{-1}; medium, K_La 10 h^{-1}; high, K_La 100 h^{-1}), in shake-flask cultures. Culture samples were taken at the mid-exponential growth phase (i.e., after 22 h). eGFP fluorescence was quantified by flow cytometry on 20,000 cells and expressed as TFU (total fluorescence; see materials and methods for calculation details). Data are means and standard deviations of triplicate cultures.

SdOE eGfp strain, with growth rate values of 0.109, 0.285, and 0.337mgDCW $(mL\,h)^{-1}$ on average under low, medium, and high OTC, respectively. Therefore, oxygen transfer was most likely a limiting factor for the growth of the FdhKO SdOE eGfp strain compared to the FdhKO eGfp strain. Under all tested culture conditions, the higher growth rate observed in the FdhKO SdOE eGfp strain compared to the FdhKO eGfp strain is due to the overexpression of *SOR1*, which allows the FdhKO SdOE eGfp strain to metabolise sorbitol at a higher rate. At the sampling time, cell growth was not limited by sorbitol availability, as it remained in excess in the culture medium (i.e., at 22 h, Figure S8).

Cells were also analysed by flow cytometry to assess both the median eGFP fluorescence and the distribution of the cell population according to eGFP fluorescence signal, distinguishing between non-induced and induced cells (i.e., with eGFP signal above a defined threshold, Theron et al. (2019)). The eGFP signal decreased as the oxygen transfer increased (i.e., 36% for FdhKO eGfp and 23% for FdhKO SdOE eGfp strains, on average) although the values did not markedly differ between the two strains for a given OTC (with a maximum of 12%) (Figure 3B). The comparable reduction in specific eGFP fluorescence observed in the FdhKO eGfp strain, despite its constant growth rate across all OTC conditions ($0.028 \pm 0.002\,h^{-1}$), rules out protein dilution as the cause of the decreased eGFP fluorescence signal in the FdhKO SdOE eGfp strain, where the growth rate increased threefold between low and high OTC. Therefore, the observed reduction in eGFP fluorescence reflects a decrease in P_{AOX1} induction.

A significant difference was observed in the fraction of the cell population in an induced state between the two strains and the culture conditions. The FdhKO SdOE eGfp strain exhibited a significantly lower fraction of the population in an induced state compared to the FdhKO eGfp strain, especially at low OTC, with a 7.8-fold difference (i.e., 5.1% vs. 39.2%, respectively; Figure 3C). The fraction of the population in an induced state also decreased significantly as oxygen transfer increased, with a 7.6-fold decrease for the FdhKO eGfp strain (i.e., 39.2% vs. 5.2%, respectively). Therefore, at low oxygen transfer, a greater portion of cells is in an induced state. This observation aligns with our previous findings of elevated *AOX1* expression levels under transient hypoxic conditions (Velastegui et al. 2023). In

experiments using a P_{AOX1}-*eGFP* strain grown on methanol, phenotypic diversification toward a highly fluorescent phenotype was observed under transient anoxic stress, with the fraction of the population in the highly fluorescent state increasing as hypoxic stress intensified.

By combining the eGFP fluorescence and the percentage of induced cells, the total fluorescence was calculated. It increased 12-fold for the FdhKO eGFP strain at low OTC compared to the high one (i.e., 105,267 and 8939 TFU, respectively). A similar trend was observed for the FdhKO SdOE eGFP strain, although to a lesser extent, with a 5-fold decrease (i.e., 12,184 and 2709 TFU, respectively). The total eGFP fluorescence signal, and thus P_{AOX1} induction, was 39-fold higher for the FdhKO eGFP strain at low OTC compared to the FdhKO SdOE eGFP strain at high OTC (i.e., 105,267 and 2709 TFU, respectively) (Figure 3D). At low OTC, the e*GFP* gene expression level for the FdhKO eGFP strain was 5.4-fold higher than for the FdhKO SdOE eGFP strain (Figure S9). According to these results, the fraction of the cell population in an induced state is greatly affected by the level of oxygen transfer as compared to the strength of induction. Strain behaviour is also influenced by the cells' ability to metabolise sorbitol (i.e., *SOR1* expression).

6.4 | Understanding the Differences in P_{AOX1} Induction Levels Between FdhKO and FdhKO-SdOE Strains Grown on Sorbitol-Based Methanol-Free Medium

In yeast, cytoplasmic formate serves as an intermediate in the THF-C1 pathway, the primary source of C1 units for *de novo* purine synthesis and energy storage molecules (e.g., adenosine triphosphate, ATP; Christensen and Mackenzie 2006, Figure S3). Disruption of the Fdh encoding gene has been identified as a key factor in intracellular formate accumulation in cells grown on sorbitol, thereby enhancing P_{AOX1} induction in a sorbitol-based methanol-free medium (Bustos et al. 2024). However, the reduced eGFP-specific fluorescence, lipase CalB and GOx activities observed in FdhKO-SdOE strains compared to their FdhKO counterparts (Figures 1 and 2) suggest that additional factors may influence P_{AOX1} induction.

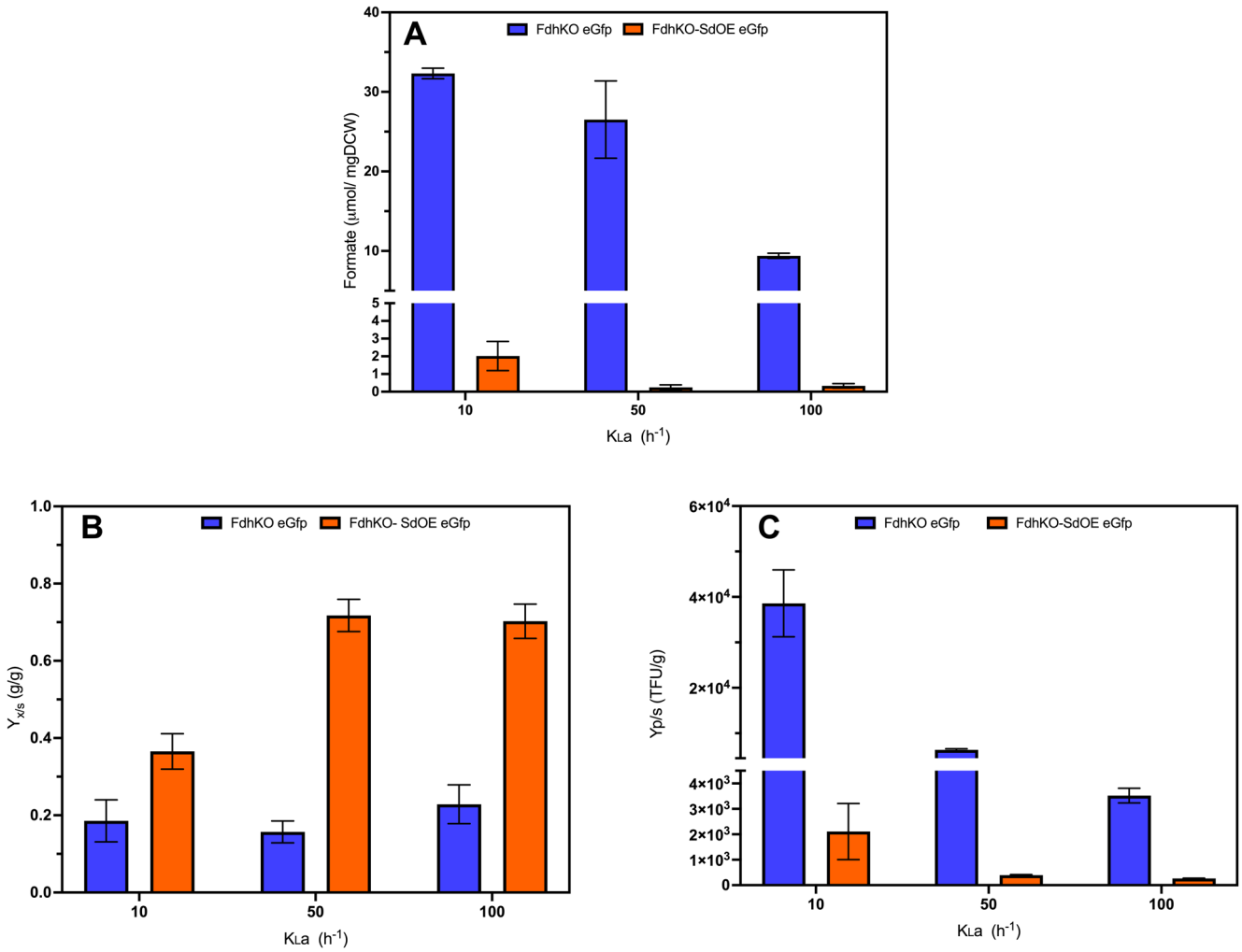

FIGURE 4 | Specific formate concentration (panel A), biomass-substrate yield coefficient ($Y_{x/s}$, panel B) and product-to-substrate yield coefficient ($Y_{p/s}$, panel C) for FdhKO eGfp (blue bars) and FdhKO-SdOE eGfp (orange bars) strains grown under different OTC, benchmarked by K_La, in shake-flask cultures. Culture samples were taken at the mid-exponential growth phase (i.e., after 22 h). Data are means and standard deviations of biological triplicate.

Overexpression of *SOR1* in FdhKO strains led to an increased sorbitol uptake rate, resulting in a higher growth rate (Table 2). This increased demand for anabolic precursors, including C1 units, likely reduces formate accumulation. To test this hypothesis, formate levels were quantified in the culture supernatants of FdhKO eGfp and FdhKO SdOE eGfp strains grown on sorbitol at different OTC. For the FdhKO SdOE eGfp strain, formate concentrations were markedly lower than for the FdhKO-eGfp strain across all tested OTC (Figure 4A). Additionally, formate content decreased for both strains as the oxygen transfer increased. For the FdhKO eGfp strain, formate concentration was 32.3 μmol mgDCW^{-1} at low OTC, whereas it was nearly undetectable for the FdhKO SdOE eGfp strain at high OTC (0.33 μmol mgDCW^{-1}). Sorbitol metabolism differs between FdhKO-eGfp and FdhKO-SdOE-eGfp strains due to *SOR1* overexpression. The FdhKO eGfp strain exhibited a low conversion efficiency of sorbitol into biomass, with a substrate-to-biomass yield coefficient ($Y_{x/s}$) ranging from 0.18 to 0.22 g g^{-1} across all tested OTC. At low OTC, the $Y_{x/s}$ of the FdhKO SdOE eGfp strain was 1.9-fold higher than that of the FdhKO eGfp (0.36 g g^{-1}), increasing further to 0.7 g g^{-1} at medium and high OTC (Figure 4B). Conversely, when considering eGFP as a product, the substrate-to-product yield coefficient ($Y_{p/s}$) for the FdhKO SdOE eGfp strain was 18-fold lower than that of the FdhKO eGfp strain at low OTC (38,586 vs. 2110 TFU g^{-1}, respectively, Figure 4C). For both strains, $Y_{p/s}$ decreased as oxygen transfer increased, with a 10.9-fold reduction between low and high OTC for the FdhKO eGfp strain (38,586 vs. 3521 TFU g^{-1}, respectively).

Elevated formate concentrations were associated with low OTC, low $Y_{x/s}$, and high $Y_{p/s}$. Under these conditions, e*GFP* gene expression for the FdhKO eGfp strain was 5.4-fold higher than under conditions of high $Y_{x/s}$ and low $Y_{p/s}$ (i.e., high OTC, Figure S8). This suggests that formate accumulation under conditions of low oxygen transfer and limited sorbitol catabolism likely stems from a reduced flux through the cytoplasmic C1-THF pathway, driven by a lower demand for de novo purine biosynthesis. In FdhKO strains lacking formate dehydrogenase, this leads to an accumulation of cytoplasmic formate, which in turn contributes to enhanced P_{AOX1} induction. This observation highlights the role of low $Y_{x/s}$, favored under low OTC, in enhancing P_{AOX1} induction.

7 | Conclusion

We recently demonstrated that *K. phaffii* FdhKO strains exhibit self-induction of the p P_{AOX1}-based expression system when grown on sorbitol. In this study, we further show that these strains undergo diauxic growth in methanol-free glycerol-sorbitol media, effectively decoupling cell growth from recombinant protein production. Under these conditions, accumulated formate from the THF-C1 metabolism triggers P_{AOX1} induction. To increase energy generation in the FdhKO strain, sorbitol catabolism was optimised by overexpression of *SOR1*. Although increased sorbitol metabolism enhances biomass formation, it simultaneously reduces P_{AOX1} induction, as evidenced by lower formate accumulation, decreased eGFP fluorescence, and reduced secreted CalB and Gox activities in *SOR1*-overexpressing strains. Oxygen transfer also modulates these dynamics, with lower oxygen availability favouring higher P_{AOX1} induction due to increased formate accumulation. Notably, the observed increase in P_{AOX1} expression appears to result from phenotypic diversification within the cell population, leading to a higher fraction of induced cells rather than an overall increase in P_{AOX1} induction per cell. These findings underscore the metabolic trade-offs in sorbitol-based processes and highlight the potential for optimising carbon flux to balance recombinant protein production and cell growth. Future studies should focus on fine-tuning metabolic pathways to enhance energy efficiency while sustaining robust P_{AOX1} induction in methanol-free, sorbitol-based media.

Author Contributions

Cristina Bustos: writing – original draft, conceptualization, investigation, formal analysis. **Rocio Cozmar:** writing – original draft, conceptualization, investigation, formal analysis. **Julio Berrios:** writing – review and editing, funding acquisition, conceptualization. **Patrick Fickers:** conceptualization, methodology, writing – review and editing, supervision, funding acquisition, formal analysis, project administration.

Acknowledgements

The authors thank L. Henrion, V. Vandenbroucke, A. Padmanabhan, Korka, S. Telek, A. Zicler, S. Steels, and R. Thomas for their technical assistance and valuable discussions. The graphical abstract was created with BioRender.com. This research was funded by Becas Doctorado Nacional grant number 21211138 and 21211350 Agencia Nacional de Investigación y Desarrollo (ANID), Chile; Doctoral Internship Scholarship (PUCV, Chile); Research Stay Scholarship (Dirección de Postgrado y Programas, UTFSM, Chile); ERASMUS+ 2022–2023 Grant agreement for mobility participants—Higher education (PIC:999854952, E10208749); Wallonie-Bruxelles International through the Cooperation bilateral Belgique-Chilli project SUB/2019/435787 (RIO4), SUB/2023/591923/MOD (RI06) and SUB/2023/585456 (RC06). FONDECYT Regular (project number 1191196), University of Liege, Terra Teaching and Research Center.

Conflicts of Interest

The authors declare no conflicts of interest.

Data Availability Statement

Data are available upon request to the corresponding author.

References

Akentyev, P., D. Sokolova, A. Korzhenkov, I. Gubaidullin, and D. Kozlov. 2023. "Expression Level of *SOR1* Is a Bottleneck for Efficient Sorbitol Utilization by Yeast Komagataella Kurtzmanii." *Yeast* 40: 414–424.

Berrios, J., C. W. Theron, S. Steels, et al. 2022. "Role of Dissimilative Pathway of *Komagataella phaffii* (*Pichia pastoris*): Formaldehyde Toxicity and Energy Metabolism." *Microorganisms* 10: 1466.

Bustos, C., J. Berrios, and P. Fickers. 2024. "Formate From THF-C1 Metabolism Induces the *AOX1* Promoter in Formate Dehydrogenase-Deficient *Komagataella phaffii*." *Microbial Biotechnology* 17: e70022.

Carly, F., H. Niu, F. Delvigne, and P. Fickers. 2016. "Influence of Methanol/Sorbitol Co-Feeding Rate on p*AOX1* Induction in a *Pichia pastoris* Mut+ Strain in Bioreactor With Limited Oxygen Transfer Rate." *Journal of Industrial Microbiology & Biotechnology* 43: 517–523.

Carnicer, M., K. Baumann, I. Töplitz, et al. 2009. "Macromolecular and Elemental Composition Analysis and Extracellular Metabolite Balances of *Pichia pastoris* Growing at Different Oxygen Levels." *Microbial Cell Factories* 8: 1–14.

Çelik, E., P. Çalık, and S. G. Oliver. 2009. "Fed-Batch Methanol Feeding Strategy for Recombinant Protein Production by *Pichia pastoris* in the Presence of Co-Substrate Sorbitol." *Yeast* 26: 473–484.

Christensen, K. E., and R. E. Mackenzie. 2006. "Mitochondrial One-Carbon Metabolism Is Adapted to the Specific Needs of Yeast, Plants and Mammals." *BioEssays* 28: 595–605.

Ergün, B. G., J. Berrios, B. Binay, and P. Fickers. 2021. "Recombinant Protein Production in *Pichia pastoris*: From Transcriptionally Redesigned Strains to Bioprocess Optimization and Metabolic Modelling." *FEMS Yeast Research* 21: foab057.

Ergün, B. G., K. Laçın, B. Çaloğlu, and B. Binay. 2022. "Second Generation *Pichia pastoris* Strain and Bioprocess Designs." *Biotechnology for Biofuels and Bioproducts* 15: 150.

Feng, A., J. Zhou, H. Mao, H. Zhou, and J. Zhang. 2022. "Heterologous Protein Expression Enhancement of *Komagataella phaffii* by Ammonium Formate Induction Based on Transcriptomic Analysis." *Biochemical Engineering Journal* 185: 108503.

Fickers, P., J. M. Nicaud, J. Destain, and P. Thonart. 2003. "Overproduction of Lipase by *Yarrowia lipolytica* Mutants." *Applied Microbiology and Biotechnology* 63: 136–142.

Gorczyca, M., J. Kaźmierczak, S. Steels, P. Fickers, and E. Celińska. 2020. "Impact of Oxygen Availability on Heterologous Gene Expression and Polypeptide Secretion Dynamics in *Yarrowia lipolytica*-Based Protein Production Platforms." *Yeast* 37: 559–568.

Hartner, F. S., and A. Glieder. 2006. "Regulation of Methanol Utilisation Pathway Genes in Yeasts." *Microbial Cell Factories* 5: 39.

Jayachandran, C., B. Palanisamy Athiyaman, and M. Sankaranarayanan. 2017. "Formate Co-Feeding Improved *Candida antarctica* Lipase B Activity in *Pichia pastoris*." *Research Journal of Biotechnology* 12: 29–36.

Jordan, P., J. Y. Choe, E. Boles, and M. Oreb. 2016. "Hxt13, Hxt15, Hxt16 and Hxt17 From *Saccharomyces cerevisiae* Represent a Novel Type of Polyol Transporters." *Scientific Reports* 6: 23502.

Liu, B., H. Li, H. Zhou, and J. Zhang. 2022. "Enhancing Xylanase Expression by *Komagataella phafi* by Formate as Carbon Source and Inducer." *Applied Microbiology and Biotechnology* 106: 7819–7829.

Lv, X., W. Yu, C. Zhang, et al. 2023. "C1-Based Biomanufacturing: Advances, Challenges and Perspestives." *Bioresource Technology* 367: 128259.

Niu, H., L. Jost, N. Pirlot, et al. 2013. "A Quantitative Study of Methanol/Sorbitol Co-Feeding Process of a *Pichia pastoris* Mut+/pAOX1-lacZ Strain." *Microbial Cell Factories* 12: 33.

Prielhofer, R., J. J. Barrero, S. Steuer, et al. 2017. "GoldenPiCS: A Golden Gate-Derived Modular Cloning System for Applied Synthetic Biology in the Yeast *Pichia pastoris*." *BMC Systems Biology* 11: 123.

Sassi, H., F. Delvigne, T. Kar, et al. 2016. "Deciphering How *LIP2* and *POX2* Promoters Can Optimally Regulate Recombinant Protein Production in the Yeast *Yarrowia lipolytica*." *Microbial Cell Factories* 15: 159.

Singh, A., and A. Narang. 2020. "The Mut+ Strain of *Komagataella phaffii* (*Pichia pastoris*) Expresses p*AOX1* 5 and 10 Times Faster Than Muts and Mut− Strains: Evidence That Formaldehyde or/and Formate Are True Inducers of p*AOX1*." *Applied Microbiology and Biotechnology* 104: 7801–7814.

Singh, A., and A. Narang. 2023. "P*AOX1* Expression in Mixed-Substrate Continuous Cultures of *Komagataella phaffii* (*Pichia pastoris*) is Completely Determined by Methanol Consumption Regardless of the Secondary Carbon Source." *Frontiers in Bioengineering and Biotechnology* 11: 1123703.

Theron, C. W., J. Berrios, S. Steels, et al. 2019. "Expression of Recombinant Enhanced Green Fluorescent Protein Provides Insight Into Foreign Gene-Expression Differences Between Mut+ and MutS Strains of *Pichia pastoris*." *Yeast* 36: 285–296.

Toivari, M. H., L. Salusjärvi, L. Ruohonen, and M. Penttilä. 2004. "Endogenous Xylose Pathway in *Saccharomyces cerevisiae*." *Applied and Environmental Microbiology* 70: 3681–3686.

Tyurin, O. V., and D. G. Kozlov. 2015. "Deletion of the *FLD* Gene in Methylotrophic Yeasts *Komagataella phaffii* and *Komagataella kurtzmanii* Results in Enhanced Induction of the *AOX1* Promoter in Response to Either Methanol or Formate." *Microbiology (N Y)* 84: 408–411.

Velastegui, E., J. Quezada, C. Altamirano, J. Berrios, and P. Fickers. 2023. "Co-Feeding Strategy Alleviates Hypoxic Stress in Large-Scale Bioreactor for Optimal Production of Secretory Recombinant Proteins in *Pichia pastoris*." *Journal of Biotechnology* 373: 20–23.

Velastegui, E., C. Theron, J. Berrios, and P. Fickers. 2019. "Downregulation by Organic Nitrogen of *AOX1* Promoter Used for Controlled Expression of Foreign Genes in the Yeast *Pichia pastoris*." *Yeast* 36: 297–304.

Supporting Information

Additional supporting information can be found online in the Supporting Information section. **Figure S1:** Sorbitol metabolism in *K. phaffii*: PpHxt1, a hexose transporter, is evaluated in this investigation as a putative sorbitol transporter; Sdh refers to sorbitol dehydrogenase. **Figure S2:** Methanol utilisation pathway in *Komagataella phaffii*. Aox1, 2: alcohol oxidase1 and 2; Cat: catalase; Das1, 2: dihydroxyacetone synthase; Fld: formaldehyde dehydrogenase; Fgh: S-formylglutathione hydrolase; Fdh: formate dehydrogenase; Dak: dihydroxyacetone kinase; Tpi: triose phosphate isomerase; Fba: fructose-1,6-bisphosphate aldolase; Fbp: fructose-1,6-bisphosphatase; GS(H): glutathione; DHA: dihydroxyacetone; DHAP: dihydroxyacetone phosphate; GAP: glyceraldehyde-3-phosphate; F1,6BP: fructose-1,6-bisphosphate; F6P: fructose-6-phosphate; Xu5P: xylulose 5-phosphate. **Figure S3:** Tetrahydrofolate (THF) mediated one-carbon (THF-C1) metabolism in yeast. Fdh, formate dehydrogenase; Shm1, mitochondrial serine hydroxymethyltransferase; Shm2, cytosolic serine hydroxymethyltransferase; Mis1-2, formate-tetrahydrofolate ligase; Mis1-3, methylenetetrahydrofolate dehydrogenase & methenyltetrahydrofolate cyclohydrolase; Mis1-1, trifunctional enzyme: formate-tetrahydrofolate ligase, methenyltetrahydrofolate cyclohydrolase and methylenetetrahydrofolate reductase; THF, tetrahydrofolate. Figure adapted from (Bustos, et al.2024). **Figure S4:** Sorbitol Dehydrogenase enzyme. Protein alignment. XP_002489933.1 corresponds to (gene PAS_chr1-1_0490) protein sequence *K. phaffii*, and XKU26523.1 corresponds to *Saccharomyces cerevisiae*. **Figure S5:** Hexose transporter protein. Protein alignment. XP_002490706.1 corresponds to (gene PAS_chr1-4_0570) protein sequence *K. phaffii*, and CAA98825.1 corresponds to *Saccharomyces cerevisiae*. **Figure S6:** Schematic representation of the genotype of yeast strains. **Figure S7:** Glycerol and sorbitol concentration during the growth of FdhKO eGfp strain (blue colours, Panel A) and FdhKO SdOE eGfp strain (orange colours, Panel B) in YNB minimal medium containing different mixtures of glycerol and sorbitol (YNBG0, 1.75 g L^{-1} glycerol; YNBGS2, 1.75 g L^{-1} glycerol and 1.75 g L^{-1} sorbitol; YNBGS4, 1.75 g L^{-1} glycerol and 3.5 L^{-1} sorbitol). The data show one representative culture. **Figure S8:** Sorbitol concentration after 22 h of growth of strains SdhKO eGfp (blue) and SdhKO SdOE eGfp (orange) in the YNBS2 medium under different OTC (low, $K_L a$ 10 h^{-1}; medium, $K_L a$ 10 h^{-1}; high, $K_L a$ 100 h^{-1}). Data are the mean and standard deviation of triplicate cultures conducted in shake flasks. **Figure S9:** e*GFP* gene expression level for FdhKO eGfp and FdhKO-SdOE eGfp strains cultured strains grown under different OTC (low, $K_L a$ 10 h^{-1}; high, $K_L a$ 100 h^{-1}), in shake-flask cultures. Culture samples were taken at the mid-exponential growth phase (i.e., after 22 h). Data are means and standard deviations of triplicate cultures. Gene expression levels were normalised according to that of actin gene. **Table S1:** mbt270263-sup-0001-DataS1.docx. *Escherichia coli* strains used in this study. **Table S2:** Primers used in this study.